

A yield-vertex modification of two-surface models of metal plasticity

H. PETRYK (WARSZAWA) and K. THERMANN (DORTMUND)

A PHENOMENOLOGICAL MODEL of elastoplastic behaviour of metal polycrystals is proposed which combines the features of micromechanical models with the classical flow theory of plasticity. The standard equation of a smooth loading surface describes here an outer limit surface which is never reached. The actual inner yield surface possesses a vertex at the current loading point, interpreted as the point of intersection of active yield surfaces for plastic flow mechanisms at a micro-level. The incremental response of the material at the vertex is defined in terms of the position of the current stress relative to the outer surface. In the computational version of the model, the effects of partial unloading and of physical and constraint hardening are represented by separate constitutive functions.

1. Introduction

THE CLASSICAL FLOW THEORY of time-independent plasticity is based on the assumption of a smooth yield surface and of a flow rule that prescribes the direction of the plastic part of strain-rate in the current state. On the contrary, micromechanical models of elastoplastic polycrystals invariably predict (cf. [1–4]) the formation of a vertex on the yield surface at the current loading point, as well as the existence of a whole range of admissible plastic strain-rate directions, the actual one being dependent on the current stress-rate.

Accordingly, two separate classes of time-independent phenomenological constitutive models for polycrystalline metals in the plastic range have been proposed: of the classical type and of the corner (or vertex) type. The former have a simpler structure in the incremental form and can in principle be constructed using the accumulated knowledge of experimental yield surfaces, while the latter are closer to micromechanical predictions and are expected to simulate better the material response after an abrupt change of the direction of straining. In calculations, the J_2 corner theory of plasticity formulated in [5] was most frequently used among relatively few phenomenological corner models proposed so far for metal polycrystals [6–14].

The purpose of this paper is to develop a phenomenological model of elastoplastic behaviour of metal polycrystals which combines the features of the above two classes of constitutive description. A *given* model of the classical type is modified in order to improve the consistency with general conclusions drawn from a micromechanical analysis [3]. Accordingly, the classical smooth yield surface plays here the role of an outer *extremal* (limit or target) surface which is

never reached, while the related inner yield surface (a boundary of the actual elastic domain) possesses a vertex at the current loading point. The extremal surface may be interpreted as a locus of *asymptotic* stress states approached when physical hardening is imagined to be suspended [3]. A considerable simplification in the proposed computational model, and also the difference in relation to the previous corner theories, is that the incremental response of the material is defined in terms of the position of the current stress point with respect to the *extremal* surface, independently of evolution of the latter, e.g. according to an isotropic/kinematic hardening law. In turn, the fundamental distinction from plasticity models with two or more loading surfaces [15–18] is that the inner surface is here no longer smooth. The derivation of the incremental law at the vertex of the inner yield surface also appears to be novel. In the first approximation, the simplest assumption of mutually independent internal mechanisms of plastic deformation at a micro-level has been explored.

2. Two-surface model of plasticity with a vertex on the inner yield surface

The small-strain formulation is given first; an extension to a geometrically exact description at finite strain will be given in Sec. 4. The standard yield condition of the Huber–Mises type:

$$(2.1) \quad \bar{\tau} = k, \quad \bar{\tau} \equiv \left(\frac{1}{2} (\boldsymbol{\sigma}' - \boldsymbol{\alpha}) \cdot (\boldsymbol{\sigma}' - \boldsymbol{\alpha}) \right)^{1/2}$$

is adopted here as an equation of the *extremal* surface in the sense of HILL [3]. $\boldsymbol{\sigma}$ denotes the Cauchy stress⁽¹⁾, $\boldsymbol{\sigma}'$ its deviator, $\boldsymbol{\alpha}$ denotes the deviatoric backstress and k is the yield shear stress. $\boldsymbol{\alpha}$ and k can vary with the plastic deformation according to prescribed rules which are left arbitrary here. (2.1) can be replaced by a more general equation of a smooth surface without changing the remaining part of this section. However, the specifications in the next section are only given for the form (2.1).

Contrary to classical elastoplasticity, the surface (2.1) is not allowed to be reached, and plastic deformation can take place when the current stress lies inside the surface (2.1). During plastic flow, the current stress point $\boldsymbol{\sigma}$ constitutes a vertex on the inner yield surface which is a boundary of the current elastic domain (Fig. 1 a). The vertex is interpreted as an intersection point of individual smooth yield surfaces (transformed to the *macroscopic* stress space) for a large or infinite number of internal plastic deformation mechanisms at a micro-level,

⁽¹⁾ In the standard symbolic notation employed, bold-face letters denote second- or fourth-order tensors, a dot between two tensor symbols denotes full contraction, a tensor product is denoted by \otimes , and $|\dot{\boldsymbol{\sigma}}| = (\dot{\boldsymbol{\sigma}} \cdot \dot{\boldsymbol{\sigma}})^{1/2}$ denotes a norm of the stress-rate. Throughout the paper, only symmetric second-order tensors are used.

cf. [3]. Such a mechanism can be identified, for instance, with crystallographic slipping on some system in some grain in a polycrystalline aggregate. We restrict ourselves to examining the case when the matrix of hardening moduli, which represents mutual interactions between the mechanisms either within the same grain or in different grains, is symmetric and positive definite. A well known consequence is that the fourth-order tensor of macroscopic plastic compliances, denoted below by \mathbf{M}^P , is diagonally symmetric and at least positive semi-definite.

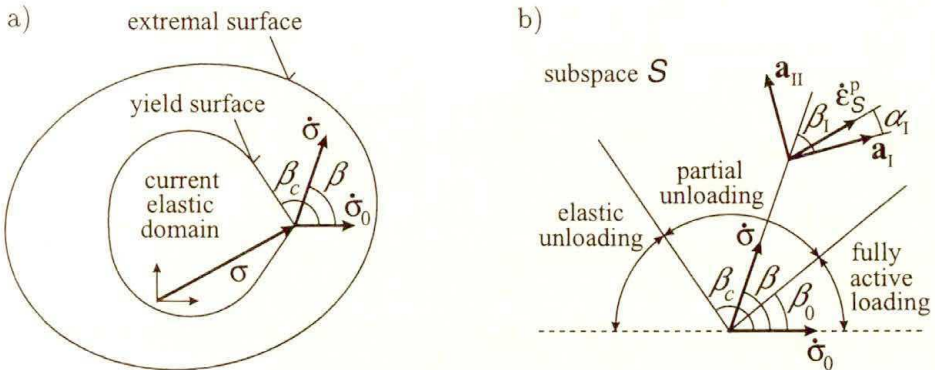


FIG. 1. (a) Two-surface model of plasticity where the inner yield surface has a vertex at the current loading point and the outer extremal surface is smooth. (b) Overall structure of the incremental plastic constitutive law at the yield-vertex, within a two-dimensional subspace \mathcal{S} .

As long as unloading is absent or partial so that the elastic domain is not penetrated, a phenomenological constitutive relationship at the vertex may be defined without specifying the entire form of the elastic domain but merely the directions tangent to the corner of the elastic domain at σ' . In a given state of the material, a macroscopic plastic strain-rate $\dot{\epsilon}^P$ is assumed to be a single-valued, positively homogeneous of degree one, continuous and (except at $\dot{\sigma} = 0$) at least piecewise-continuously differentiable function of a macroscopic stress-rate $\dot{\sigma}$. It is emphasized that a dot over a symbol denotes the *forward* rate. We will examine that function restricted to a two-dimensional subspace \mathcal{S} of the Euclidean space of symmetric second-order tensors, and denote by $\dot{\epsilon}_S^P$ the orthogonal projection $\mathbf{P}_S \cdot \dot{\epsilon}^P$ on $\mathcal{S}^{(2)}$. By the Euler theorem, the homogeneous incremental plastic law can be written down as

$$(2.2) \quad \begin{aligned} \dot{\epsilon}^P &= \mathbf{M}^P(\dot{\sigma}) \cdot \dot{\sigma}, & \mathbf{M}^P &= \frac{\partial \dot{\epsilon}^P}{\partial \dot{\sigma}}, \\ \dot{\epsilon}_S^P &= \mathbf{M}_S^P(\dot{\sigma}) \cdot \dot{\sigma}, & \mathbf{M}_S^P &= \mathbf{P}_S \mathbf{M}^P \mathbf{P}_S, \quad \text{if } \dot{\sigma} \in \mathcal{S}. \end{aligned}$$

The diagonal symmetry of \mathbf{M}^P implies that \mathbf{M}_S^P is a diagonally symmetric operator within \mathcal{S} . From the spectral decomposition theorem for fourth-order

(²) If (\mathbf{a}, \mathbf{b}) with $\mathbf{a} \cdot \mathbf{b} = 0, |\mathbf{a}| = |\mathbf{b}| = 1$ is an orthonormal basis in \mathcal{S} then $\mathbf{P}_S = \mathbf{a} \otimes \mathbf{a} + \mathbf{b} \otimes \mathbf{b}$.

diagonally symmetric tensors (cf. [19]), we obtain that \mathbf{M}_S^p , henceforth assumed to be positive definite, has the following representation

$$(2.3) \quad \begin{aligned} \mathbf{M}_S^p &= M_I \mathbf{a}_I \otimes \mathbf{a}_I + M_{II} \mathbf{a}_{II} \otimes \mathbf{a}_{II}, \\ \mathbf{a}_I, \mathbf{a}_{II} &\in \mathcal{S}, \quad \mathbf{a}_I \cdot \mathbf{a}_{II} = 0, \quad |\mathbf{a}_I| = |\mathbf{a}_{II}| = 1, \end{aligned}$$

with principal directions $\mathbf{a}_I, \mathbf{a}_{II}$ and positive principal compliances M_I, M_{II} . Let $\dot{\boldsymbol{\sigma}}_0 \neq \mathbf{0}$ define a distinctive direction within \mathcal{S} , and β denote an angle of inclination of a nonzero $\dot{\boldsymbol{\sigma}}$ to $\dot{\boldsymbol{\sigma}}_0$,

$$(2.4) \quad \cos \beta = \frac{\dot{\boldsymbol{\sigma}} \cdot \mathbf{a}_0}{|\dot{\boldsymbol{\sigma}}|}, \quad \mathbf{a}_0 = \frac{\dot{\boldsymbol{\sigma}}_0}{|\dot{\boldsymbol{\sigma}}_0|}.$$

The considerations below are limited to $\dot{\boldsymbol{\sigma}} \in \mathcal{S}$ lying on one side of $\dot{\boldsymbol{\sigma}}_0$ where $\beta \in [0, \pi]$; the other side can be examined analogously.

Each quantity in (2.3) depends in general on β . An admissible function $\mathbf{M}_S^p(\beta)$, if discontinuous, must ensure the continuity of $\dot{\boldsymbol{\epsilon}}_S^p(\dot{\boldsymbol{\sigma}})$, and at every differentiability point it must satisfy the additional condition

$$(2.5) \quad \frac{d\mathbf{M}_S^p}{d\beta} \cdot \dot{\boldsymbol{\sigma}} = \mathbf{0}$$

obtained by differentiation of (2.2). On substituting (2.3), the condition (2.5) is easily transformed to

$$(2.6) \quad \begin{aligned} \frac{dM_I}{d\beta} \cos \beta_I &= \left(\frac{d\beta_I}{d\beta} - 1 \right) (M_I - M_{II}) \sin \beta_I, \\ \frac{dM_{II}}{d\beta} \sin \beta_I &= \left(\frac{d\beta_I}{d\beta} - 1 \right) (M_I - M_{II}) \cos \beta_I, \end{aligned}$$

where β_I is an angle between $\dot{\boldsymbol{\sigma}}$ and \mathbf{a}_I with

$$(2.7) \quad \cos \beta_I = \frac{\dot{\boldsymbol{\sigma}} \cdot \mathbf{a}_I}{|\dot{\boldsymbol{\sigma}}|}, \quad \sin \beta_I = \frac{\dot{\boldsymbol{\sigma}} \cdot \mathbf{a}_{II}}{|\dot{\boldsymbol{\sigma}}|}.$$

From (2.3) we also find that β_I is connected with an angle α_I between $\dot{\boldsymbol{\epsilon}}_S^p$ and \mathbf{a}_I through

$$(2.8) \quad \tan \alpha_I = \frac{M_{II}}{M_I} \tan \beta_I.$$

It can be seen that if *one* scalar function from the triple $\{M_I(\beta), M_{II}(\beta), \beta_I(\beta)\}$ defining $\mathbf{M}_S^p(\beta)$ is prescribed then the two other have to satisfy two differential

equations (2.6), with appropriate boundary conditions. That restriction is related to the existence of a stress-rate potential $\Psi^P(\dot{\sigma})$,

$$(2.9) \quad \dot{\epsilon}^P = \frac{\partial \Psi^P}{\partial \dot{\sigma}}, \quad \Psi^P = \frac{1}{2} \dot{\epsilon}^P \cdot \dot{\sigma} \quad \text{and} \quad \Psi^P = \frac{1}{2} \dot{\sigma} \cdot \mathbf{M}_S^P \cdot \dot{\sigma} \quad \text{if } \dot{\sigma} \in \mathcal{S},$$

which is a consequence of the diagonal symmetry of \mathbf{M}^P . If more than one scalar constitutive function in a subspace \mathcal{S} is assumed, as in [12, 14], then the potentiality property is generally lost.

Further considerations are restricted to the case $0 < \beta_1 < \pi/2$ illustrated in Fig. 1 b. Moreover, we will assume that $M_{I-II} \equiv M_I - M_{II} > 0$ and that $0 < d\beta_1/d\beta \leq 1$. Then (2.6) holds if and only if either

$$(2.10) \quad \frac{d\beta_1}{d\beta} = 1, \quad \frac{dM_I}{d\beta} = 0, \quad \frac{dM_{II}}{d\beta} = 0,$$

or

$$(2.11) \quad \frac{d\beta}{d\beta_1} - 1 \equiv r \in (0, \infty),$$

$$\frac{dM_I}{d\beta_1} = -r M_{I-II} \tan \beta_1, \quad \frac{dM_{II}}{d\beta_1} = -r M_{I-II} \cot \beta_1.$$

In the former case $\mathbf{M}_S^P(\beta) = \text{const}$. In the second case, the following differential equation for M_{I-II} is obtained:

$$(2.12) \quad \frac{dM_{I-II}}{d\beta_1} = 2r M_{I-II} \cot 2\beta_1.$$

This defines a class of constitutive relationships corresponding to different functions $r(\beta_1)$. A particular solution

$$(2.13) \quad M_{I-II} = 2\bar{M} \sin^r 2\beta_1$$

is obtained for r independent of β_1 , with $\bar{M} > 0$ being a positive integration constant.

Suppose that there exists a stress-rate $\dot{\sigma}_0$ codirectional with the principal direction of $\mathbf{M}^P(\dot{\sigma}_0)$ associated with the *maximum* principal plastic compliance; in particular, $\dot{\sigma}_0$ is then codirectional with $\dot{\epsilon}^P(\dot{\sigma}_0)$. To cover all directions in the stress-rate space, it suffices to consider the two-dimensional subspaces \mathcal{S} that contain $\dot{\sigma}_0$ as the common distinctive stress-rate used to determine the angle β from (2.4). If \mathbf{M}_S^P varies continuously with β then from (2.10) and (2.11) it follows that the principal plastic compliances $M_I(\beta)$, $M_{II}(\beta)$ are non-increasing functions which attain maximum values at $\beta = \beta_1 = 0$. If (2.10) holds for $\beta < \beta_0$, say, then that interval of β can be identified with the angular range of fully active loading

in the current state, while an interval of validity of (2.11), $\beta_0 < \beta < \beta_c$ say, can be identified with the transitory range of partial unloading, cf. [3]. We shall assume that $(-\dot{\boldsymbol{\sigma}}_0)$ lies within the current elastic unloading cone corresponding to $\beta_c < \beta \leq \pi$, cf. Fig. 1 b.

To derive a constitutive function in the transitory range rather than to define it arbitrarily, we propose the following simplifying procedure. The effect of physical hardening within the grains in a polycrystalline aggregate is included into a hardening rule for the *extremal* surface, e.g. into an evolution rule for $\boldsymbol{\alpha}$ and k in (2.1). The interaction (in the stress-space formulation) between micro-mechanisms of plastic deformation in different grains is imagined to be represented, at least partially, by variations of \overline{M} inside the extremal surface (see below). Finally, a phenomenological relationship between the plastic strain-rate and stress-rate at the vertex on the inner yield surface, which includes the effect of partial unloading, is constructed as for mutually independent mechanisms of plastic deformation. For comparison, in the well-known theories of BATDORF and BUDIANSKY [1] or KOITER [6], the effects of interaction between the plastic deformation mechanisms were fully neglected, while here they are taken into account in an indirect manner.

Under that assumption, the range of fully active loading becomes a prolongation of the elastic unloading range, so that $\beta_0 = \pi - \beta_c$. Both ranges suffer a *right-hand* discontinuous change in time if $\dot{\boldsymbol{\sigma}}$, the current right-hand rate of stress, induces partial unloading. Then, $\dot{\boldsymbol{\sigma}}$ constitutes one limiting ray of the *new* angular range of fully active loading⁽³⁾, while the second limiting ray of that range is regarded as varying continuously in time. The key simplifying assumption is that $\mathbf{a}_1(\beta)$ corresponding to any direction of loading (total or partial) within \mathcal{S} always bisects the *right-hand limit* (in time) of the angular range of elastic unloading. It follows that in the range of partial unloading, \mathbf{a}_1 rotates continuously with increasing β so that (cf. (2.13))

$$(2.14) \quad r = 1, \quad M_{I-II} = 2\overline{M} \sin 2\beta_1,$$

with a parameter \overline{M} independent of β_1 . It may be noted that (2.14) gives $d(M_I + M_{II})/d\beta_1 = -4\overline{M}$. To obtain a smooth transition to elastic unloading, we assume that M_I tends to zero as $\beta \rightarrow \beta_c$. On using the condition of continuity of $\dot{\boldsymbol{\epsilon}}_S^P(\dot{\boldsymbol{\sigma}})$, we obtain the following solution to (2.11) in the transition range:

$$(2.15) \quad \begin{aligned} \beta \in [\beta_0, \beta_c], \quad \beta_c = \pi - \beta_0, \quad \beta_1 = \frac{1}{2}(\pi - \beta_c + \beta) = \frac{1}{2}(\beta_0 + \beta), \\ M_I = (\pi - 2\beta_1 + \sin 2\beta_1)\overline{M}, \quad M_{II} = (\pi - 2\beta_1 - \sin 2\beta_1)\overline{M} \end{aligned}$$

⁽³⁾ Fully active loading means that each plastic deformation mechanism that is potentially active (i.e. stressed to its yield point in the current state) is actually active. After partial unloading, some of previously potentially active mechanisms become inactive, so that the angular range of fully active loading increases discontinuously. For infinitely many mechanisms, $\dot{\boldsymbol{\sigma}}$ corresponding to partial unloading will generally induce neutral loading for some mechanism(s), i.e. will constitute the limiting ray as stated above; cf. also [20].

and in the range of fully active loading:

$$(2.16) \quad \begin{aligned} \beta &\in [0, \beta_0], & \beta_I &= \beta, \\ M_I &= (\pi - 2\beta_0 + \sin 2\beta_0)\overline{M}, & M_{II} &= (\pi - 2\beta_0 - \sin 2\beta_0)\overline{M}. \end{aligned}$$

For convenience, the basic relationship between M_I , M_{II} and β_0 or β_I for fully or partially active loading, respectively, is visualized in Fig. 2.

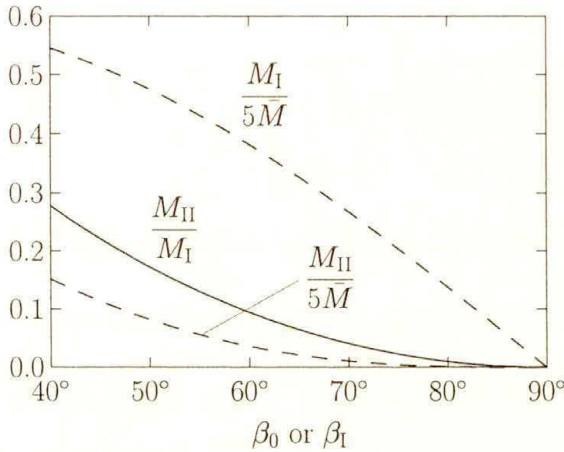


FIG. 2. Principal plastic compliance ratio, M_{II}/M_I , as a function of β_0 for fully active loading or of β_I after partial unloading. Broken lines show the respective variations of the principal plastic compliances scaled down by $5\overline{M}$.

From elementary geometry it follows that $\dot{\epsilon}_S^P$ makes an angle $(\pi - \beta_I - \alpha_1)$ or $(\pi - \beta_0 - \alpha_1)$ in the range of partially or fully active loading, respectively, with the limiting ray of the elastic unloading range in the respective subspace \mathcal{S} , cf. Fig. 1 b. It can be checked by using (2.8), (2.15) and (2.16) that this angle decreases monotonically from β_c to $\pi/2$ as β increases from zero to β_c . Hence, $\dot{\epsilon}_S^P$ lies within the range generated by the outward normals to the limiting rays of the elastic unloading range in \mathcal{S} , in agreement with the generalized normality rule at a yield-surface vertex.

Once the elastic unloading cone in $\dot{\sigma}$ -space has been specified in the current state, then the elastic unloading range within each \mathcal{S} is known along with its internal angle $2\beta_0$, external angle $2\beta_c$ and outward bisector \mathbf{a}_0 . Finally, the constitutive relationship between $\dot{\epsilon}^P$ and $\dot{\sigma}$ is fully determined, after substituting (2.15) and (2.16) into (2.3) and next into (2.9), by the geometry of the current elastic unloading cone and by the scalar parameter \overline{M} dependent on the material state and on \mathcal{S} . Of course, when performing the partial differentiation in (2.9), the dependence of the parameters \overline{M} and β_0 on the subspace \mathcal{S} must be taken into account in general. That dependence is absent from the simplest version of the model discussed in the next section.

3. A simple computational version of the model

Suppose first that the current state of the material has been reached by proportional loading from a virgin unstressed state with $\alpha = 0$; this condition will later be relaxed. Under the usual assumption of an incompressible and pressure-insensitive plastic flow, the following specifications (cf. Fig. 3) are made in the incremental constitutive law from Sec. 2:

(i) The deviatoric stress-rate space and its two-dimensional subspace \mathcal{S}' are substituted in place of $\dot{\sigma}$ -space and \mathcal{S} .

(ii) The elastic unloading cone has a symmetry axis codirectional with $(\sigma' - \alpha)$, and β is defined by (2.4) with

$$(3.1) \quad a_0 = \frac{\sigma' - \alpha}{|\sigma' - \alpha|}.$$

(iii) The parameters β_0 and \overline{M} are independent of \mathcal{S}' and depend on the placement of σ' relative to the extremal surface.

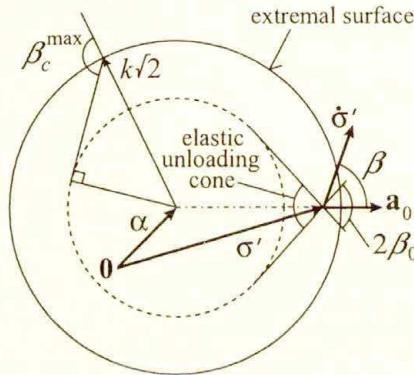


FIG. 3. Construction of the elastic unloading cone in the computational version of the two-surface model.

The relationship between the plastic strain-rate and stress-rate at the vertex σ' on the inner yield surface becomes fully defined by two state-dependent scalar parameters β_0 and \overline{M} being functions of the current values of α , k and σ' . In the potential form, the incremental plastic constitutive law is given by

$$(3.2) \quad \dot{\epsilon}^P = \frac{\partial \Psi^P}{\partial \dot{\sigma}}, \quad \Psi^P = \frac{1}{2} F(\beta) |\dot{\sigma}'|^2,$$

$$(3.3) \quad F(\beta) = \overline{M} \cdot \begin{cases} \pi - 2\beta_0 + \sin 2\beta_0 \cos 2\beta & \text{for } 0 \leq \beta \leq \beta_0 \quad (\text{total loading}), \\ \pi - (\beta + \beta_0) + \frac{1}{2} \sin 2(\beta + \beta_0) & \text{for } \beta_0 \leq \beta \leq \pi - \beta_0 \quad (\text{partial unloading}), \\ 0 & \text{for } \pi - \beta_0 \leq \beta \leq \pi \quad (\text{total unloading}). \end{cases}$$

In an explicit form, it reads⁽⁴⁾

$$\begin{aligned}
 \dot{\boldsymbol{\epsilon}}^P &= \overline{M}(A(\beta)|\dot{\boldsymbol{\sigma}}'| \mathbf{a}_0 + B(\beta)\dot{\boldsymbol{\sigma}}'), \\
 \left. \begin{aligned}
 A(\beta) &= 2 \cos \beta \sin 2\beta_0, \\
 B &= \pi - 2\beta_0 - \sin 2\beta_0
 \end{aligned} \right\} & \text{for } \beta \leq \beta_0, \\
 (3.4) \quad \left. \begin{aligned}
 A(\beta) &= \sin^2(\beta + \beta_0)/\sin \beta, \\
 B(\beta) &= \pi - (\beta + \beta_0) - \sin \beta_0 \sin(\beta + \beta_0)/\sin \beta
 \end{aligned} \right\} & \text{for } \beta_0 \leq \beta \leq \pi - \beta_0, \\
 \left. \begin{aligned}
 A &= 0, \\
 B &= 0
 \end{aligned} \right\} & \text{for } \pi - \beta_0 \leq \beta \leq \pi.
 \end{aligned}$$

This can be complemented by the standard equation for the elastic part of strain-rate, viz.

$$(3.5) \quad \dot{\boldsymbol{\epsilon}} = \dot{\boldsymbol{\epsilon}}^e + \dot{\boldsymbol{\epsilon}}^P, \quad \dot{\boldsymbol{\epsilon}}^e = \mathbf{M}^e \cdot \dot{\boldsymbol{\sigma}},$$

with \mathbf{M}^e being the compliance tensor of the linear theory of isotropic elasticity.

Finally, specification of the parameters β_0 and \overline{M} and of evolution equations for k and $\boldsymbol{\alpha}$ completes the set of constitutive equations of the model. The evolution rule for the extremal surface is left arbitrary here since the equations are proposed as a refinement of a given model of the classical type. β_0 and \overline{M} are assumed to depend on the relative distance of the current deviatoric stress $\boldsymbol{\sigma}'$ from the extremal surface. For instance, they can be expressed in terms of the ratio $\bar{\tau}/k$ as

$$(3.6) \quad \beta_0 = \arcsin \frac{k \sin \beta_c^{\max}}{\bar{\tau}}, \quad \frac{\bar{\tau}}{k} \in (\sin \beta_c^{\max}, 1), \quad \beta_c^{\max} = \text{const} \in \left(\frac{\pi}{2}, \pi\right),$$

$$(3.7) \quad \overline{M}(\beta_0) = \frac{1}{E} \frac{2}{1 - \chi(\beta_0)/\chi(\pi - \beta_c^{\max})}, \quad \chi(\beta_0) = \frac{\pi - 2\beta_0 - \sin 2\beta_0}{\sin \beta_0},$$

where β_c^{\max} is a material constant and E is the elastic Young modulus. In comparison with the standard elastoplastic model, that specification of the yield-vertex modification requires only one additional material constant β_c^{\max} . Formula (3.6) means that generators of the elastic unloading cone are tangent to a sphere with centre $\boldsymbol{\alpha}$ and radius $k\sqrt{2} \sin \beta_c^{\max}$ in $\boldsymbol{\sigma}'$ -space, cf. Fig. 3. During proportional loading in the range $\bar{\tau}/k \leq \sin \beta_c^{\max}$, we substitute $\overline{M} = 0$ with β_0 undefined. On the other hand, the inner sphere shown in Fig. 3 by a broken line is only used to

⁽⁴⁾ A closer inspection of Eq. (3.4) shows a resemblance to the equation obtained in [9] in a different way and without considering its potential form. The present equation is more general since \overline{M} is a function of state rather than a constant. The distinction is essential since constant \overline{M} would be inconsistent with the existence of a fixed unattainable extremal surface when physical hardening within the grains is suspended. To have consistency, $1/\overline{M}$ must tend to zero when a fixed extremal surface is approached.

define the current elastic unloading cone at $\boldsymbol{\sigma}'$ and need not be identified with the boundary of the current elastic domain.

The function (3.7) has been chosen to fit approximately the tensile stress/plastic strain curves calculated for micromechanical models of a polycrystal [4]; the approximation will further be discussed in the next section. Of course, one could also take another function \overline{M} in place of (3.7) to obtain a better fit of micromechanical results. The present choice was influenced by the convenient possibility of determining analytically the plastic strain under proportional loading from the unstressed virgin state if the extremal surface is fixed. From (3.6) with fixed k and from (2.16) we obtain the interesting formula

$$(3.8) \quad \frac{M_I}{\overline{M}} d\bar{\tau} = d\left(\frac{M_{II}}{\overline{M}} \bar{\tau}\right).$$

On using (3.6) and the definition of χ in (3.7), the plastic strain under proportional loading is thus given by

$$(3.9) \quad \boldsymbol{\epsilon}^P = \mathbf{a}_0 \sqrt{2} \int_0^{\bar{\tau}} M_I d\bar{\tau} = \mathbf{a}_0 k \sqrt{2} \sin \beta_c^{\max} \int_0^{\chi} \overline{M} d\chi.$$

This motivates the use of \overline{M} expressed in terms of χ . The form (3.7)₁ is one of the simplest which ensure $\overline{M} \rightarrow \infty$ as $\bar{\tau}$ approaches a fixed k ; after integration it yields

$$(3.10) \quad \boldsymbol{\epsilon}^P = \mathbf{a}_0 \frac{2k\sqrt{2}}{E} (2\beta_c^{\max} - \pi + \sin 2\beta_c^{\max}) \ln \frac{1}{1 - \chi(\beta_0)/\chi(\pi - \beta_c^{\max})}$$

with β_0 determined from (3.6) for a fixed extremal surface.

In turn, from (3.9), (3.6) and the definition of χ we obtain

$$(3.11) \quad \boldsymbol{\epsilon}^P = M_{II} \boldsymbol{\sigma}' \quad \text{if } \overline{M} = \text{const}.$$

This is precisely the formula of the classical *deformation* theory of plasticity where the proportionality factor between the plastic strain and stress deviators, being a function of $|\boldsymbol{\sigma}'|$, serves as the principal plastic compliance for $\boldsymbol{\sigma}'$ orthogonal to $\boldsymbol{\sigma}'$. In view of a fixed relationship between M_{II} and $|\boldsymbol{\sigma}'|$ implied by (2.16) and (2.6), the variant of the deformation theory obtained here for fully active loading at constant \overline{M} is very special and, moreover, inconsistent with the assumption of a fixed extremal surface. The possibility to satisfy Eq. (3.11) *approximately* for the extremal surface subject to a power hardening law will be discussed in Sec. 5.

The assumption (ii) above, and hence the final specification of the incremental plastic constitutive law, cannot be regarded as appropriate for all stress-rates in all states, e.g. in the current state just after partial unloading. Fortunately, to

calculate the material response along some loading path, it usually suffices to know the function $\dot{\epsilon}^P(\dot{\sigma})$ only in the vicinity of the *actual* stress-rate direction. For a class of non-proportional loading paths, the actual plastic strain-rate and plastic compliances can be calculated from (3.3), or directly from (3.4) and (2.15) or (2.16), respectively, still by using the specifications (i)–(iii) in the following cases:

(A) for every stress-rate in any state \mathcal{P}_A reached from a virgin state $\sigma' = \mathbf{0}$, $\alpha = \mathbf{0}$ along a plastic straining path without unloading (i.e. with $\beta \leq \beta_0$ in the range $\bar{\tau}/k > \sin \beta_c^{\max}$, except in the current state \mathcal{P}_A itself);

(B) along any path starting from a state \mathcal{P}_A and such that σ' and α are being contained in a fixed two-dimensional deviatoric subspace and β is preserving its sense, nondecreasing (but possibly discontinuous) in time and satisfying $\beta < \beta_c$;

(C) along any straight path in the deviatoric stress space starting from \mathcal{P}_A and satisfying $\beta < \beta_c$;

(D) along any smooth path of a sufficiently small curvature in the deviatoric stress space, starting from \mathcal{P}_A and satisfying $\beta < \beta_c$.

This can be inferred from the assumptions under which the equations of the computational model have been derived. The common condition in the above list is that no elastic unloading takes place so that the current stress does not leave the vertex on the inner yield surface. This condition could be weakened by allowing for elastic unloading not followed by reloading, and also for certain cases of reloading. The restriction on the path curvature in point (D) is imprecise since it is difficult to specify the circumstances in which the influence of partial unloading on the *actual* tangent compliances along a curved path may still be neglected. A curvature of the order $1/k$ may perhaps be regarded as being “sufficiently small” in this respect.

4. Extension to finite strain

The extension of the constitutive equations from the preceding sections to plastic strain of arbitrary magnitude can be done in the following way, regarded nowadays as standard. With the volume changes assumed to be purely elastic and small, σ is replaced by the Kirchhoff stress $\tau = J\sigma$ where J is the current-to-reference volume ratio, while the stress-rate $\dot{\sigma}$ is replaced by $\overset{\nabla}{\tau}$, the Zaremba–Jaumann flux (corotational with the material spin) of τ . An exact elastic constitutive law can be defined as an isotropic linear relationship between the back-rotated Kirchhoff stress and logarithmic elastic strain relative to an unstressed state. Accordingly, the elastic compliances of the linear theory of isotropic elasticity undergo a slight modification, cf. [21]. $\dot{\epsilon}$ is identified with the Eulerian strain-rate \mathbf{D} while its plastic part \mathbf{D}^P is defined by (3.5) and determined from (3.2) or (3.4) after making the substitutions indicated. A finite strain

problem can be analysed in the usual step-by-step manner if, in every traversed state, \mathbf{D} as an invertible function of $\overset{\nabla}{\boldsymbol{\tau}}$ is specified at least in the vicinity of the actual incremental solution.

Questions resulting from the multiplicative decomposition of the deformation gradient and concerning the effect of plastic rotations on the kinematic hardening law need not be addressed here since they do not affect the proposed modification of a *given* classical plasticity model.

5. Illustrative examples

Figures 4–7 illustrate the model behaviour during proportional loading from an unstressed virgin state, by the representative example of uniaxial tension. The tensile stress σ is scaled down by $\sigma_0 = k_0\sqrt{3}$, the initial tensile yield stress in the absence of the yield-vertex modification, i.e. for the classical model. The tensile plastic strain ε^P is normalized by the elastic critical strain σ_0/E . Figure 4 shows how the stress varies with the plastic strain for the classical model (the horizontal line) and for $\beta_c^{\max} = 105^\circ, 120^\circ, 130^\circ$ and 139.2° when the extremal surface is kept fixed. This case corresponds to perfect plasticity within the grains of a polycrystal, where the increase of the macroscopic stress is due to “constraint hardening”. The curves can be compared with the results given in [4] for micromechanical models of a polycrystal. The lowest curve in Fig. 4 for $\sin \beta_c^{\max} = \sin 139.2^\circ \approx 1/1.53$ corresponds to an upper bound of the constraint hardening effect (cf. [3, 4]) and, after suitable rescaling, fits approximately the results obtained from the Kröner–Budiansky–Wu self-consistent model. Fitting the results obtained in [4] for Hill’s self-consistent model, regarded as more accurate, would require a somewhat smaller value of β_c^{\max} . Identification of an optimal

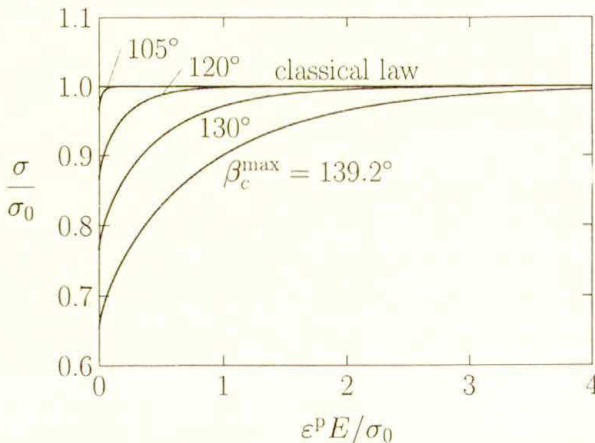


FIG. 4. Non-dimensional stress vs. plastic strain in uniaxial tension for a fixed extremal surface and for different values of β_c^{\max} .

value of β_c^{\max} is not straightforward since the yield-surface corner angle in a phenomenological model should be interpreted as an *effective* angle obtained when an unspecified plastic strain due to some internal mechanisms is neglected. For otherwise, the assumption of the existence of a finite elastic domain at advanced plastic deformation could be questioned; cf. the remark in [4], p. 271.

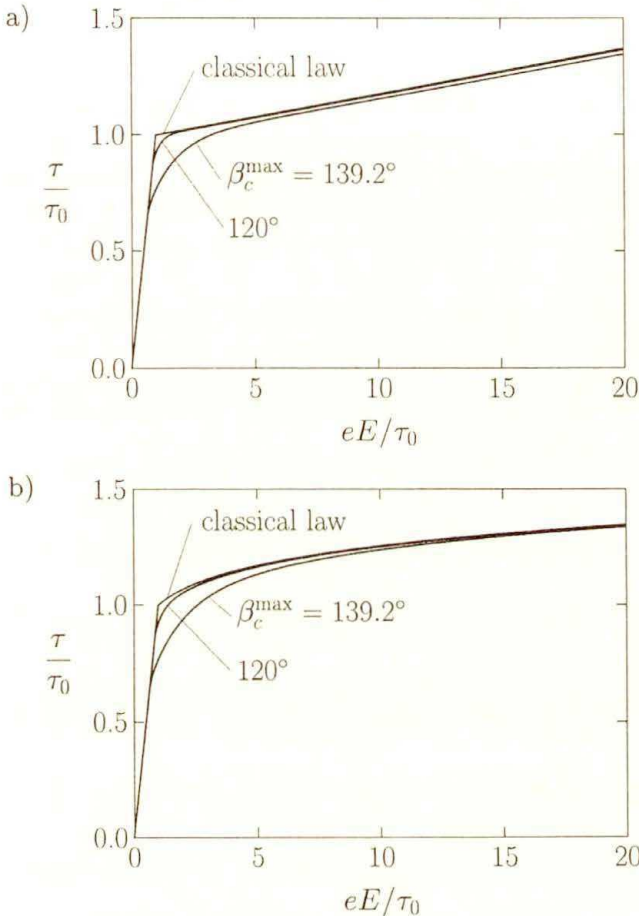


FIG. 5. Uniaxial Kirchhoff stress τ as a function of logarithmic strain e for the extremal surface subject to an isotropic, (a) linear $\tau = k\sqrt{3} = \tau_0 + 0.02Ee^p$, or (b) power hardening law $\tau = \tau_0(1 + e^p E/\tau_0)^{0.1}$, for different values of β_c^{\max} .

The results in Fig. 5 correspond to the extremal surface being not fixed but subject to an isotropic linear or power hardening law. The finite strain version described in Sec. 4 has been employed, with τ_0 as the uniaxial Kirchhoff stress on the initial extremal surface and $\tau = (e - e^p)E$. It can be seen that the uniaxial stress-strain curve for the classical law is closely approximated by the curves for the present model when the plastic strain becomes only a few times greater than the elastic strain. However, the difference is no longer fully negligible even

for larger strains, especially for linear hardening with a constant modulus h (equal to $0.02E$ in Fig. 5 a). The reason is that an asymptotic value β_0^∞ of β_0 is now somewhat greater than $(\pi - \beta_c^{\max})$. It can be found from the condition $d\beta_0/de^P = 0$ which leads to the relationship

$$(5.1) \quad \sin \beta_0^\infty - \frac{2}{3}hM_1(\beta_0^\infty) \sin \beta_c^{\max} = 0.$$

While the yield-vertex modification of a stress-strain curve for proportional loading at advanced plastic strain may be regarded as insignificant, the corresponding difference in the incremental constitutive law is substantial. This is illustrated in Fig. 6 where plots of the effective tangent shear modulus vs. loading angle after tensile prestrain are presented for different values of β_c^{\max} . The plots correspond to a fixed extremal surface in the small strain formulation, and the amount of plastic prestrain for each value of β_c^{\max} corresponds to the same relative distance to the extremal surface, defined by $(1 - \bar{\tau}/k)/(1 - \sin \beta_c^{\max}) = (1 - 1.3/1.53)/(1 - 1/1.53)$ to allow comparison with the similar Fig. 6 in [4]. The calculated effective tangent shear modulus in the total loading range tends at $\beta_c^{\max} \rightarrow \pi/2$ to the elastic shear modulus G , i.e. to the value obtained for the flow theory of plasticity.

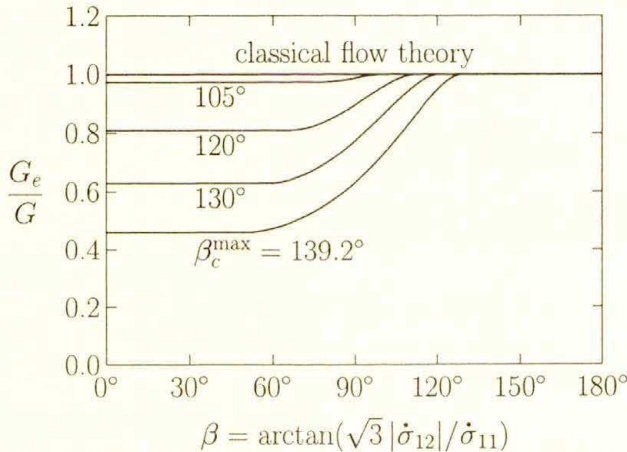


FIG. 6. Effective tangent shear modulus $G_e = \dot{\sigma}_{12}/2\dot{\epsilon}_{12}$ as a function of the incremental loading angle β after tensile prestrain corresponding to a given relative distance (see the text) to a fixed extremal surface. $G = E/2(1 + \nu)$ is the elastic shear modulus with $\nu = 0.3$.

The difference between the incremental characteristics for the present and classical models is also illustrated in Fig. 7. Plots of the principal plastic compliance ratio M_{II}/M_I vs. strain in uniaxial tension are shown for $\beta_c^{\max} = 120^\circ$ and 135° while for the classical plasticity law the ratio is identically zero. Solid lines correspond to a linear isotropic, broken lines to a power-type isotropic, and

dotted lines to a linear kinematic hardening law for the extremal surface. The material parameters for the isotropic hardening correspond to Figs. 5 a and 5 b, and the kinematic hardening law is specified by $\dot{\alpha} = (2/3)(0.01E)\mathbf{D}^p$. It can be seen that the value of M_{II}/M_I is only slightly influenced by the type of hardening, and also by the amount of strain beyond a certain initial stage. On the other hand, the ratio depends strongly on the value of β_c^{\max} . This is, of course, not surprising since this ratio depends only on β_0 as illustrated in Fig. 2. Figure 7 may thus be treated as another illustration of the conclusion that during proportional loading at advanced plastic deformation, when the current hardening modulus is much smaller than E , the value of $\beta_c = \pi - \beta_0$ is close to β_c^{\max} and hence almost constant.

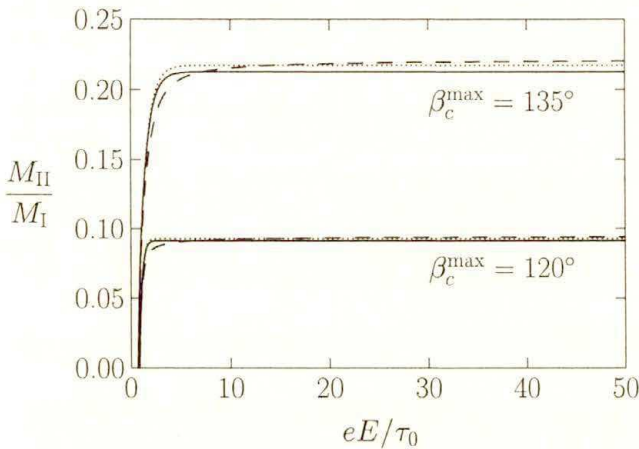


FIG. 7. Variation of principal plastic compliance ratio M_{II}/M_I with logarithmic strain in uniaxial tension for the extremal surface subject to a linear isotropic ———, power-type isotropic - - - and linear kinematic hardening law for two values of β_c^{\max} . Isotropic hardening parameters as in Fig. 5, kinematic hardening law $\dot{\alpha} = (2/3)(0.01E)\mathbf{D}^p$.

A stabilized value of the ratio of the principal plastic compliances resembles the well-known property of the deformation theory of plasticity obeying a power hardening law. In the small-strain formulation with the elastic strain neglected, M_{II}/M_I under proportional loading becomes then equal to the tangent-to-secant modulus ratio, and hence to the constant power exponent. The present model can approximate such behaviour provided β_c^{\max} is appropriately selected, with the help of the relationship visualized in Fig. 2, to give the required value of the compliance ratio. The power hardening exponent corresponding to β_c^{\max} equal to 120° or 135° can be directly read off as a stabilized ordinate in Fig. 7.

It is beyond the scope of this paper to simulate the material response for various paths of non-proportional loading, which is expected to be strongly influenced by the choice of an isotropic/kinematic hardening rule for the extremal

surface. We recall that the proposed yield-vertex modification does not restrict the freedom in selecting such a hardening rule that fits experimental data for a specified material.

6. Concluding remarks

A modification of the family of classical models for plastically deforming metals has been obtained with the help of general conclusions drawn from micromechanical analysis of an elastic-plastic polycrystal. In comparison with the standard equations of the flow theory of plasticity, the proposed model in its simplest computational version involves only one additional material constant which defines the maximal sharpness of the corner at the current loading point on the inner yield surface. A smooth loading surface of the standard form has been used as an outer "extremal" surface [3], not attainable during plastic flow. With the yield-vertex effect included, the high (elastic) stiffness of the classical elastic-plastic model against an abrupt change of the straining direction has been relaxed. This offers a perspective of more adequate modelling of the material behaviour under non-proportional loading, and of arriving at more realistic results in bifurcation and instability studies, still using a typical isotropic/kinematic hardening law for the outer loading surface.

References

1. S.B. BATDORF and B. BUDIANSKY, *A mathematical theory of plasticity based on the concept of slip*, NACA TN, No. 1871, 1949.
2. T.H. LIN, *A proposed theory of plasticity based on slips*, Proc. 2nd U.S. Nat. Congr. Appl. Mech., pp. 461–468, ASME, Ann Arbor 1954.
3. R. HILL, *The essential structure of constitutive laws for metal composites and polycrystals*, J. Mech. Phys. Solids, **15**, 79–95, 1967.
4. J.W. HUTCHINSON, *Elastic-plastic behaviour of polycrystalline metals and composites*, Proc. Roy. Soc. Lond., **A 319**, 247–272, 1970.
5. J. CHRISTOFFERSEN and J.W. HUTCHINSON, *A class of phenomenological corner theories of plasticity*, J. Mech. Phys. Solids, **27**, 465–487, 1979.
6. W.T. KOITER, *Stress-strain relations, uniqueness and variational theorems for elastic-plastic materials with a singular yield surface*, Quart. Appl. Math., **11**, 350–353, 1953.
7. J.L. SANDERS, *Plastic stress-strain relations based on linear loading functions*, Proc. 2nd U.S. Nat. Congr. Appl. Mech., pp. 455–460, ASME, Ann Arbor 1954.
8. B. BUDIANSKY, *A reassessment of deformation theories of plasticity*, ASME J. Appl. Mech., **26**, 259–264, 1959.
9. V.D. KLUSHNIKOV, *On a possible way of constructing the plastic deformation laws* [in Russian], Prikl. Mat. Mekh., **23**, 282–291, 1959.
10. V.D. KLUSHNIKOV, *An analytical theory of plasticity* [in Russian], Izv. AN SSSR Mekhanika, No. 2, 82–87, 1965.
11. M.J. SEWELL, *A plastic flow at a yield vertex*, J. Mech. Phys. Solids, **22**, 469–490, 1974.

12. M. GOTOH, *A class of plastic constitutive equation with vertex effect – I, II*, Int. J. Solids Structures, **21**, 1101–1116, 1117–1129, 1985.
13. Y. TOMITA, A. SHINDO, Y.S. KIM and K. MICHUURA, *Deformation behaviour of elastic-plastic tubes under external pressure and axial load*, Int. J. Mech. Sci., **28**, 263–274, 1986.
14. M. GOYA and K. ITO, *An expression of elastic-plastic constitutive law incorporating vertex formation and kinematic hardening*, ASME J. Appl. Mech., **58**, 617–622, 1991.
15. A. PHILLIPS and R.L. SIERAKOWSKI, *On the concept of the yield surface*, Acta Mech., **1**, 29–35, 1965.
16. Z. MRÓZ, *On the description of anisotropic work-hardening*, J. Mech. Phys. Solids, **15**, 163–175, 1967.
17. Y.F. DAFALIAS and E.P. POPOV, *A model of nonlinearly hardening materials for complex loading*, Acta Mech., **21**, 173–192, 1975.
18. K. HASHIGUCHI, *Constitutive equations of elastoplastic materials with elastic-plastic transition*, ASME J. Appl. Mech., **47**, 266–272, 1980.
19. J. RYCHLEWSKI, *On thermoelastic constants*, Arch. Mech., **36**, 77–95, 1984.
20. H. PETRYK, *On constitutive inequalities and bifurcation in elastic-plastic solids with a yield-surface vertex*, J. Mech. Phys. Solids, **37**, 265–291, 1989.
21. R. HILL, *Constitutive inequalities for isotropic elastic solids under finite strain*, Proc. Roy. Soc. Lond., **A 314**, 457–472, 1970.

POLISH ACADEMY OF SCIENCES

INSTITUTE OF FUNDAMENTAL TECHNOLOGICAL RESEARCH

e-mail: hpetryk@ippt.gov.pl

and

DORTMUND UNIVERSITY

DEPARTMENT OF MECHANICAL ENGINEERING, DORTMUND, GERMANY.

Received March 21, 1997.
